Ultra-Long-Range Dual Rotman Lenses-based Harmonic mmID's for 5G/mm-Wave IoT Applications

Charles A. Lynch III[#1], Ajibayo O. Adeyeye[#], Aline Eid[#], Jimmy Hester[$2], Manos M. Tentzeris[#]
[#]ATHENA Lab, Georgia Institute of Technology, USA
[$]Atheraxon, USA
[1]clynch19@gatech.edu, [2]jimmy.hester@atheraxon.com

***Abstract*— For the first time, the authors propose a Rotman Lenses-based Harmonic mmID tag topology featuring an ultra-long interrogation range for future 5G/mm-Wave IoT. The proposed system also displays a wide-angular coverage with a $-8.5\,\mathrm{dB}$ beamwidth of $\pm 45^\circ$, a harmonic RCS of $-37.4\,\mathrm{dBsm}$, while demonstrating the longest reported range of passive harmonic mmID systems. Additionally, the lens-based system provides a theoretical x9.6 range extension compared to the reported state-of-the-art in fully-passive doubler mmID systems. With a theoretical maximum range of $560\,\mathrm{m}$ with 5G/mm-Wave EIRP of $75\,\mathrm{dBm}$, this system presents a paradigm shift in ultra-long-range, fully-passive 5G/mm-Wave IoT systems.**

***Keywords*— 5G, millimeter-Wave, Rotman lens, IoT, Chip-less mmID, Long-range, Harmonic mmID**

I. Introduction

With the proliferation of Internet-of-Things (IoT), next-generation, data-driven Wireless Sensor Networks (WSNs) are expected to support over of 75 billion devices by 2025 that would typically require a proportional amount of batteries to be charged and/or replaced continuously, increasing maintenance and environmental costs of these systems. That issue establishes the need for long-range energy autonomous sensor nodes to meet the demand of these WSNs. One choice of such energy autonomous technologies is Radio-Frequency Identification (RFID) or millimeter-wave Identification (mmID) which enables fully-passive operation with various implementations, namely chip-based, chipless, and harmonic-based. Chip-based RFIDs provide the best performance in terms of range and amount of encoded information, but are the most complex design and costly to produce while featuring limited interrogation range set by the chip. Either limiting the range to the harvesting range set by the chip power threshold sensitivity in [1] or requiring some form of energy harvesting circuit, such as a solar cell in [2]. Chipless implementations have provided the simplest and cheapest solution, but are limited to a maximum range of $30\,\mathrm{m}$ shown in [3] and are only able to encode frequency or magnitude of the backscattered response. Harmonic-based mmIDs provide a good balance in complexity, range, and encoding information for tracking and sensing applications shown in [4],[5], [6],[7], and [8]. The concept behind harmonic RFID/mmID relies on the use of two distinct frequency bands: the reader to tag downlink at f_o or the fundamental frequency, and the tag to reader uplink at nf_o or the n^{th} harmonic of the fundamental frequency. By backscattering a harmonic multiple back to the reader, the clutter and self-interference of the reader are drastically reduced allowing for extended operational range.

The longest range reported chip-based and chipless implementations utilize two aspects yet to be demonstrated in harmonic mmID systems, specifically mm-Wave operation frequency, allowing higher Equivalent Isotropic Radiated Power (EIRP),and retro-directive structures, either a Rotman lens in [2] or a Van-Atta Array in [3], to focalize the backscatter signal in the direction of the interrogator. The choice of retro-directive structures was crucial due to the conversion loss (CL) of the doubler circuit in a harmonic RFID/mmID being proportional to the input power into the doubler circuit. In [9], the authors demonstrated a Rotman lens-based rectenna provided more input power at each rectifier circuit because of the passive beamforming network of the lens. Therefore, a harmonic mmID system based on dual Rotman lenses would outperform that of a harmonic mmID based on Van-Atta Array. Thus, the authors propose, for the first time, a fully-passive ultra-long range, dual Rotman Lens-based Harmonic mmID with the schematic of the mmID shown in Figure 1. The proposed system operates at $14/28\,\mathrm{GHz}$ utilizing two Rotman Lenses operating at the fundamental and first harmonic frequencies providing maintained angular coverage while demonstrating the longest reported range of a harmonic mmID system.

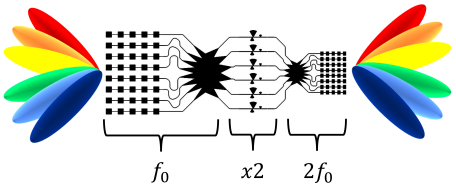

Fig. 1. Schematic of the lens-based ultra-long range wide-angular coverage harmonic mmID.

II. Long-range Harmonic mmID

The proposed ultra-long-range lens-based harmonic mmID is comprised of two sub-components namely the harmonic Rotman lenses with their associated antenna arrays in the two utilized frequency bands as well as a miniaturized frequency doubler circuit. By combining the passive beam forming network (BFN) of the Rotman lenses and the doubler circuit, the fully-passive mmID enables ultra-long-range, wide angular coverage, and improved reader sensitivity for 5G-enabled smart city applications in IoT.

A. Dual Frequency Rotman lenses

As aforementioned, to overcome the gain-coverage trade-off, a passive BFN device is utilized at the RFID tag for the reception of the interrogator signal of the interrogator,

2022 IEEE/MTT-S International Microwave Symposium - IMS 2022 | 978-1-6654-9613-1/22/$31.00 ©2022 IEEE | DOI: 10.1109/IMS37962.2022.9865357

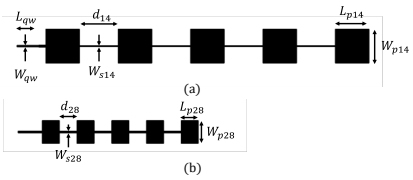

Fig. 2. (a) Schematic of 14 GHz 5×1 antenna array with $L_{qw} = 3.51\,\text{mm}$, $W_{qw} = 0.24\,\text{mm}$, $L_{p14} = W_{p14} = 5.38\,\text{mm}$, $d_{14} = 6.19\,\text{mm}$, and $W_{s14} = 0.16\,\text{mm}$. (b) Schematic of 28 GHz 5×1 antenna array with $L_{p28} = 2.74\,\text{mm}$, $W_{p28} = 3.60\,\text{mm}$, $d_{28} = 2.8\,\text{mm}$, and $W_{s28} = 0.30\,\text{mm}$.

centered at f_0, and transmission of the first harmonic centered at $2f_0$. As presented in [10], a scalability analysis of the trade-off between the array factor (AF) and angular coverage based on the number of beam and antenna ports for Rotman lenses displayed an optimal combination of 8 antenna and 6 beam ports for the best compromise. Thus, each Rotman lens was designed to have 8 antenna and 6 beam ports with a designed AF of $5.95\,\text{dB}$ and maximum angular coverage of $\pm 60°$. The mmID was designed on Rogers 4350B (ϵ_r= 3.55,$\tan\delta$ =0.027) with a thickness of $0.168\,\text{mm}$ with all components simulated in CST Microwave Studio. The footprint of the $14/28\,\text{GHz}$ Rotman lenses are $4.98\,\text{cm} \times 5.34\,\text{cm}$ and $2.52\,\text{cm} \times 2.68\,\text{cm}$, respectively. A 5×1 series-fed, linear patch antenna array was placed at each of the eight antenna ports of both the $14\,\text{GHz}$ and $28\,\text{GHz}$ Rotman lenses. The fabricated antenna arrays with labeled dimensions are shown in Figure 2. Each antenna in simulation provides an estimated gain of $10\,\text{dBi}$ with each antenna's S_{11} measuring below $-10\,\text{dB}$ over a $140\,\text{MHz}$ bandwidth centered at $13.94/27.88\,\text{GHz}$ providing good radiation efficiency for receiving fundamental and re-radiating the first harmonic back to the interrogator.

B. Frequency Doubler

As mentioned in the introduction, the frequency doubler, capable of producing harmonics at very low input power levels, should theoretically achieve longer ranges compared to rectifying chips that require a minimum amount of power to turn on and power the tag. For the design of the doubler circuit, a similar circuit architecture to [8] was utilized. The doubler circuit consists of three parallel stubs namely, an input matching stub, an open circuit stub at f_0, and a short circuit parallel stub at f_0. The input matching stub and the open circuit stub at the input of the diode provide maximum input power into the diode. Additionally, the open circuit stub at f_0 appears as a short circuit to any $2f_0$ signal that reflects to the input of the diode. The parallel short circuit stub at f_0 at the output of the diode suppresses the fundamental frequency and improves the conversion loss (CL) calculated through the input power at f_0 minus the output power of the diode at $2f_0$ and is the primary figure of merit of frequency doublers. The diode selected for the proposed proof-of-concept design is the SMS201, flip-chip, schottky diode from Macom, due to its high sensitivity, resulting in better CL. The presented doubler circuit was simulated in ADS and was measured utilizing the signal

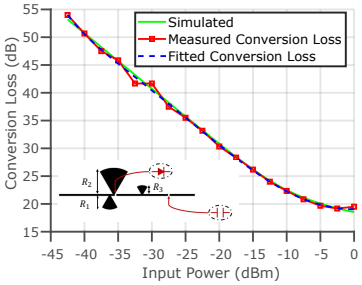

Fig. 3. The simulated, measured, and 8^{th} order polynomial fit Conversion Loss (CL) along with the circuit layout of the $14/28\,\text{GHz}$ Frequency Doubler with $R_1 = 3.55\,\text{mm}$, $R_2 = 6.55\,\text{mm}$, and $R_3 = 2.18\,\text{mm}$.

generator and spectrum analyzer. The simulated, measured, and a fitted 8^{th} order polynomial CL is displayed in Figure 3 with the doubler circuit shown in the bottom left corner. The doubler circuit efficiently doubles for input power levels as low as $-45\,\text{dBm}$, providing acceptable CL performance, all while requiring no external bias, enabling fully-passive operation.

III. Proof-of-Concept System Evaluation

Having all the subsystems designed, a proof-of-concept prototype of a fully-passive dual Rotman lens harmonic mmID, shown in Figure 1, was fabricated with an evaluation of both angular coverage and ultra-long-range interrogation.

A. Angular Coverage Evaluation

An evaluation of the angular coverage of the dual Rotman lens harmonic mmID was conducted through measuring the normalized received power of the mmID versus the angle of incidence of the interrogating signal. The harmonic mmID was placed on a stepper motor and rotated over $\pm 90\,°$ in steps of $5\,°$ with the received power level recorded at each step at a close range of $1.5\,\text{m}$ from the reader for precise measurement alignment purposes, but the broad angular coverage performance is highly scalable for ultra-long-range interrogation. A plot of this angular sweep is shown in Figure 4. The lens-based harmonic mmID displays a $-8.5\,\text{dB}$ beamwidth of $\pm 45\,°$ highlighting the exceptional angular coverage of the proposed mmID. A null at the $0\,°$ is observed due to the even number of beam ports selected for the design. This can easily overcome by adjusting the beamports to an odd number and focalizing incoming EM wave at $0\,°$ while sacrificing AF gain from the passive BFN.

B. Ultra-long Range Demonstration

To demonstrate the ultra-long-range capabilities of the proposed design, the dual Rotman-lenses based harmonic mmID was interrogated utilizing a signal generator, a $1\,\text{W}$ Power Amplifier Module (PAM), a low pass filter -to reduce harmonics generated from the PAM, which would result in self-interference-that is then connected to a $25\,\text{dBi}$ standard gain horn antenna for a measured EIRP of $51\,\text{dBm}$ operating at $14\,\text{GHz}$. For the reception of the backscattered harmonic signal, a $19.5\,\text{dBi}$ octave horn antenna was utilized. The received signal passes through a high-pass filter to reduce harmonic coupling from the Tx antenna, then is amplified by

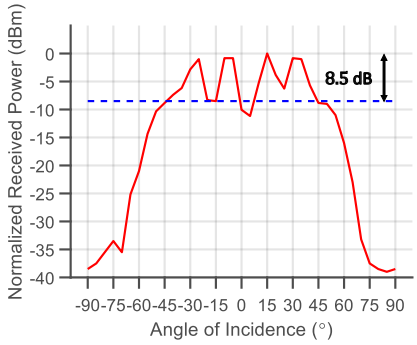

Fig. 4. Measured received normalized power of the dual lens-based fully-passive harmonic mmID versus angle of incidence at 1.5 m.

Fig. 5. Experimental setup for long-range demonstration of a proof-of-concept fully passive lens-enabled mmID at 65 m.

a 20 dB Low-Noise Amplifier (LNA) to improve the reader sensitivity, and is finally measured on a spectrum analyzer. The experimental setup of the entire system can be viewed in Figure 5. Given the above reader component specifications and a sampling rate of 30 Hz, the measured sensitivity of the reader is $-131\,\mathrm{dBm}$ for a noise spectral density of $-173.8\,\frac{\mathrm{dBm}}{\mathrm{Hz}}$. With the proof-of-concept ultra-long-range reader assembled, the fully-passive harmonic mmID was interrogated from $5\,\mathrm{m}$ to $65\,\mathrm{m}$ in steps of $5\,\mathrm{m}$ with the received power spectral density recorded at each step. The results of this measurement along with an empirical path loss exponent (EPLE) of -3.4, approximately double that of the cited EPLE from [2] for an indoor environment caused by the relationship between CL and input power into the doubler circuit, are displayed in Figure 6, highlighting its ultra-long range capabilities. Thus, to the authors knowledge, demonstrating the longest recorded range in harmonic mmID in the literature. Two metrics were used to determine the performance of the proposed system, namely maximum reading range and a harmonic radar cross-section (RCS) @ $5\,\mathrm{m}$ defined as $\sigma_{RCS_{nf_0}} = \frac{G_{f_0} G_{nf_0} \lambda_{nf_0}^2 CE_{@5\,\mathrm{m}}}{4\pi}$, where G_{f_0}, G_{nf_0}, λ_{nf_0}, and $CE_{@5\,\mathrm{m}}$, are the fundamental antenna gain, harmonic antenna gain, wavelength of the harmonic frequency, and conversion efficiency assumed to be the -CL for the input power at $5\,\mathrm{m}$ from the reader. With these two figures of merit, the dual Rotman lens-based harmonic mmID outperforms the next best system by a $13.4\,\mathrm{dB}$ in terms of harmonic RCS. Thus, presenting an order of magnitude improvement to harmonic mmID's detectability while maintaining an angular coverage of $\pm 45\,^\circ$. Additionally, with the available max EIRP of $75\,\mathrm{dBm}$ that is allowable in

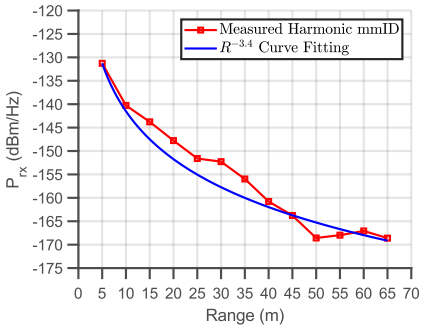

Fig. 6. Measured received power spectral density of the fully-passive dual lenses-based harmonic mmID against $R^{-3.4}$ curve fitting results for EIRP equal to $51\,\mathrm{dBm}$.

5G systems and maintaining the same reader sensitivity, a maximum reading range of the system of $560\,\mathrm{m}$ is expected. In Table 1, one can view the comparison of the multiple passive doubler RFID based systems. If the other proposed works were to scale their system in size to increase their detectability—and thus their RCS—the angular coverage would be sacrificed, a problem that was fully overcome in our solution using the cascaded harmonic Rotman lenses.

Table 1. Comparison of passive long range doubler RFID/mmID systems where * and ** denote EIRP's of $51\,\mathrm{dBm}$ and $75\,\mathrm{dBm}$, respectively.

Ref.	Frequency	EIRP	$\sigma_{RCS_{nf_0}}$	Range
[8]	2.45/4.9 GHz	25 dBm	−57.6 dBsm	5 m
[5]	3.5/7 GHz	41.7 dBm	−50.8 dBsm	7 m
[4]	5.9/11.8 GHz	42.1 dBm	−58.4 dBsm	58 m
This Work	14/28 GHz	51 dBm	−37.4 dBsm	65*/560 m**

IV. Conclusion

For the first time, a cascaded lens-based harmonic mmID tag for ultra-long-range and wide-angular coverage operation is presented. The fully-passive mmID displayed a harmonic RCS of $-37.4\,\mathrm{dBsm}$ and a $-8.5\,\mathrm{dB}$ beamwidth of ± 45 providing both high RCS with wide angular coverage. While the physical dimensions of the proposed system is relatively large, the current system presents a fully-passive mmID that could enable ubiquitous, long-range localized sensing applications, through encoding sensing information of the amplitude and frequency of the mmID. In terms of maximum reading range, the dual-lens-based system was estimated to have a maximum reading range of $65\,\mathrm{m}$ for a proof-of-concept EIRP level of $51\,\mathrm{dBm}$, establishing the longest reported range for a passive harmonic mmID system. Furthermore, with the $75\,\mathrm{dBm}$ EIRP allowable at 5G, a reading range of $560\,\mathrm{m}$ (9.6-fold increase) can be envisioned, resulting in the longest range fully-passive harmonic RFID ever-reported, and presenting a paradigm shift for future 5G/mm-Wave IoT systems. Lastly, this harmonic dual-lens-based mmID can be miniaturized through designing the fundamental frequency in the mm-Wave/5G band and doubling to B5G/6G frequencies. Thus, providing a miniaturized fully-passive, harmonic mmID architecture to link mm-Wave/5G systems the next-generation 6G systems for future IoT systems.

REFERENCES

[1] C. Occhiuzzi, A. Rida, G. Marrocco, and M. Tentzeris, "Rfid passive gas sensor integrating carbon nanotubes," *IEEE Transactions on Microwave Theory and Techniques*, vol. 59, no. 10, pp. 2674–2684, 2011.

[2] A. Eid, J. G. D. Hester, and M. M. Tentzeris, "Rotman lens-based wide angular coverage and high-gain semipassive architecture for ultralong range mm-wave rfids," *IEEE Antennas and Wireless Propagation Letters*, vol. 19, no. 11, pp. 1943–1947, 2020.

[3] J. G. D. Hester and M. M. Tentzeris, "Inkjet-printed flexible mm-wave van-atta reflectarrays: A solution for ultralong-range dense multitag and multisensing chipless rfid implementations for iot smart skins," *IEEE Transactions on Microwave Theory and Techniques*, vol. 64, no. 12, pp. 4763–4773, 2016.

[4] D. Psychoudakis, W. Moulder, C.-C. Chen, H. Zhu, and J. L. Volakis, "A portable low-power harmonic radar system and conformal tag for insect tracking," *IEEE Antennas and Wireless Propagation Letters*, vol. 7, pp. 444–447, 2008.

[5] X. Gu, N. N. Srinaga, L. Guo, S. Hemour, and K. Wu, "Diplexer-based fully passive harmonic transponder for sub-6-ghz 5g-compatible iot applications," *IEEE Transactions on Microwave Theory and Techniques*, vol. 67, no. 5, pp. 1675–1687, 2018.

[6] V. Palazzi, F. Alimenti, P. Mezzanotte, G. Orecchini, and L. Roselli, "Analysis of a multi-node system for crack monitoring based on zero-power wireless harmonic transponders on paper," in *2018 IEEE Topical Conference on Wireless Sensors and Sensor Networks (WiSNet)*, 2018, pp. 92–95.

[7] P. Li, Z. An, L. Yang, P. Yang, and Q. Lin, "Rfid harmonic for vibration sensing," *IEEE Transactions on Mobile Computing*, vol. 20, no. 4, pp. 1614–1626, 2021.

[8] V. Palazzi, F. Alimenti, P. Mezzanotte, G. Orecchini, and L. Roselli, "Zero-power, long-range, ultra low-cost harmonic wireless sensors for massively distributed monitoring of cracked walls," in *2017 IEEE MTT-S International Microwave Symposium (IMS)*. IEEE, 2017, pp. 1335–1338.

[9] A. Eid, J. Hester, and M. M. Tentzeris, "A scalable high-gain and large-beamwidth mm-wave harvesting approach for 5g-powered iot," in *2019 IEEE MTT-S International Microwave Symposium (IMS)*, 2019, pp. 1309–1312.

[10] A. Eid, J. G. Hester, and M. M. Tentzeris, "5g as a wireless power grid," *Scientific Reports*, vol. 11, no. 1, pp. 1–9, 2021.